ELSEVIER

Polymer 42 (2001) 2193–2199

polymer

www.elsevier.nl/locate/polymer

Temperature-dependent phase behavior in poly(ϵ-caprolactone)–epoxy blends

Jyh-Luen Chen, Feng-Chih Chang*

National Chiao-Tung University, Institute of Applied Chemistry, Hsinchu 30050, Taiwan, ROC

Received 17 January 2000; received in revised form 29 May 2000; accepted 21 June 2000

Abstract

The cured morphologies of poly(ϵ-caprolactone)/epoxy (PCL/epoxy) blends are examined by SEM micrographs. The phase separation mechanism of the blend can be deduced from cured morphologies influenced by the blend compositions and curing conditions. The LCST phase diagram is proposed for the system and the location of the critical point shifts with the curing temperature, which results in the change of phase separation mechanism. The curing rate promoted by higher curing temperature also influences the morphologies of the blends. The fraction of the epoxy-rich macrophase resulted from the long-distance diffusion decreases with the increase of the curing temperature. In contrast, the domain size of the epoxy microphase increases with the curing temperature, which cannot be dominated by the epoxy curing rate.

Keywords: Epoxy; Poly(ϵ-caprolactone); Phase separation

1. Introduction

In heterogeneous thermoplastic/epoxy blends, the miscibility varies with the epoxy molecular weight and results in phase separation during process of curing reaction. The phase transformation involves onset of phase separation, gelation, fixation of the dimension of phase-separated structure, end of phase separation, and vitrification [1]. During process of phase transformation, the morphology of the blend is determined by the competition between the rate of curing and rate of phase separation [2,3]. Phase separation is inhibited when the blend is at high viscosity, gelation, or vitrification, and results in none or incomplete phase separation. The diffusion rate becomes the dominant factor on the finally cured morphology. In our previous study on phenoxy/epoxy blends [3], the curing rate was promoted by a catalyst and a series of homogeneous and heterogeneous products were achieved with various degrees of phase separation.

The assessment of phase separation mechanism on the exclusive basis of scattering behavior must be made with caution [4]. The use of a microscopy can provide visual information on complicated morphological changes during process of phase separation. Phase separation process in thermoplastic/epoxy blends has been studied extensively [5–7], the spinodal decomposition (SD), the nucleation and growth (NG), or the mixed mode of both can occur. Temperature-dependent phase behavior can be studied by the morphologies of the blends at different curing temperatures [6]. When the blend mixture is homogeneous at lower temperature and becomes heterogeneous at higher temperature, the lower critical solution temperature (LCST) behavior can be concluded. The epoxy conversion at which the phase separation initiates at different temperatures can also be utilized to characterize the phase behavior [7]. For example, higher epoxy conversion of phase separation at higher temperature indicates better miscibility at high temperature, thus the upper critical solution temperature (UCST) behavior is concluded. Both LCST and UCST behaviors can be interpreted by the equation-of-state theory [8,9] where the interaction parameter is divided into three parts: segmental interaction, free volume effect contributing to the LCST behavior, and size effect contributing to the UCST behavior.

Poly(ϵ-caprolactone) (PCL) is miscible with several amine-cured epoxy resins [10–12], but two-phase morphology was observed in PCL/anhydride-cured epoxy blends [11]. The observed miscibility difference can be interpreted as the presence of hydroxyl groups in the amine-cured epoxy. These hydroxyl groups are capable of forming hydrogen bonds with the PCL ester groups. In this study,

* Corresponding author. Tel.: +886-35-712-121; fax: +886-35-723-764.
E-mail address: changfc@cc.ntcu.edu.tw (F.-C. Chang).

0032-3861/01/$ - see front matter
PII: S0032-3861(00)00511-5

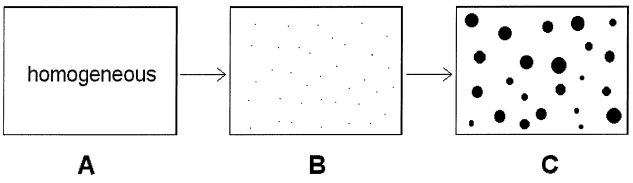

Scheme 1.

the morphologies of PCL/epoxy blends cured at different temperatures are examined by SEM. Temperature-dependent phase behavior is examined by the morphology evolution of the blends cured at different temperatures.

2. Experimental

2.1. Materials

The epoxy monomer, DER 332, was purchased from Dow Chemical Company which is a low molecular weight liquid diglycidyl ether of bisphenol-A (DGEBA) with an epoxide equivalent weight of 172–176. PCL used in this study is TONE® Polymer P-787 purchased from Union Carbide Corporation with $\bar{M}_n = 80,000$ g/mol. The aromatic amine used as a hardener is 4,4′-diaminodiphenyl sulphone (DDS) from Merck Co. The chemical structures of DGEBA, PCL, and DDS are illustrated as follows:

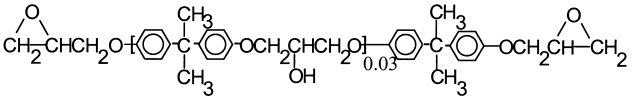

DGEBA (DER 332)

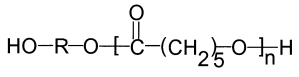

PCL

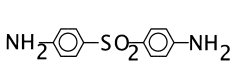

DDS

Where "R" represents an aliphatic segment in PCL structure.

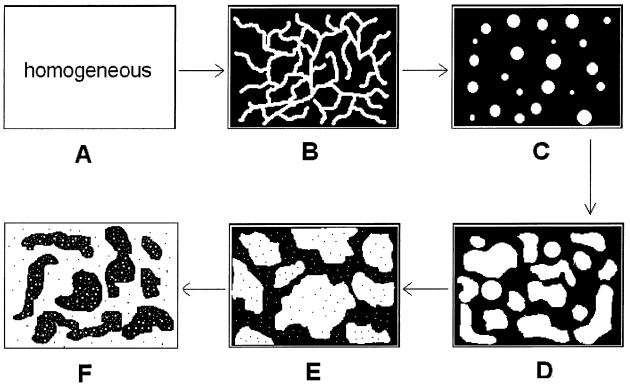

Scheme 2.

2.2. Blending procedures and characterizations

The homogeneous mixture of PCL/DGEBA = 30/70 wt% was prepared by adding PCL pellets to the stirring epoxy resin at 150°C under nitrogen gas for 1 h. Then the calculated amount of additional epoxy resin and hardener were added to bring the mixture at a desired composition. The mixture was then cast immediately into steel molds and heated at 130–170°C for 5 h. A Hitachi model S-570 scanning electronic microscopy (SEM) was employed to examine morphologies of the fracture surfaces of cured specimens.

3. Results and discussion

3.1. Phase separation process

In our previous study on PCL/epoxy blends [6], phase separation process at 150°C can be illustrated by Schemes 1 and 2. In the PCL9 blend (PCL/DGEBA/DDS = 9/67.5/22.5), PCL is segregated from the matrix by the NG mechanism (Scheme 1). For blends containing higher PCL content (PCL12 and PCL15 blends), phase separation proceeds the SD mechanism of the epoxy (Schemes 2A–C) and results in small epoxy particles dispersed in the matrix (Scheme 2C). These epoxy particles grow further and connect to each others to give the epoxy-rich macrophase domains with irregular shape (Schemes 2C–E). In the meantime, small epoxy particles appear in the PCL-rich macrophase, while the PCL small particles also appear within the epoxy-rich macrophase (Scheme 2E). After that, phase inversion occurs and the epoxy-rich phase becomes the continuous phase. At the same time, this epoxy microphase in the PCL-rich dispersed macrophase grows in size, and newer epoxy microphase with even smaller in size appears along with the original epoxy domains (Scheme 2F). This phenomenon involves complicated secondary phase separation process within the PCL-rich phase that was discussed in details in our previous report [6]. In the following sections, phase separation mechanisms of the blends will be based in Schemes 1 and 2.

3.2. Cured morphologies of the PCL9 blends

Fig. 1 displays the finally cured SEM micrographs taken on the fractured surfaces of the PCL9 blends cured from 130°C (Fig. 1a) to 170°C (Fig. 1e), respectively. In this magnification (2000×), Fig. 1a displays a typical homogeneous morphology and Fig. 1b–e displays the spherical PCL domains. The PCL domain size increases with increasing of the curing temperature (from Fig. 1b–e). Therefore, the phase separation of the PCL9 blend follows the NG mechanism as shown in Scheme 1. The LCST behavior of this blend system [6] implies that phase separation at higher curing temperature should take place at a relatively lower epoxy conversion. Therefore, the conversion interval

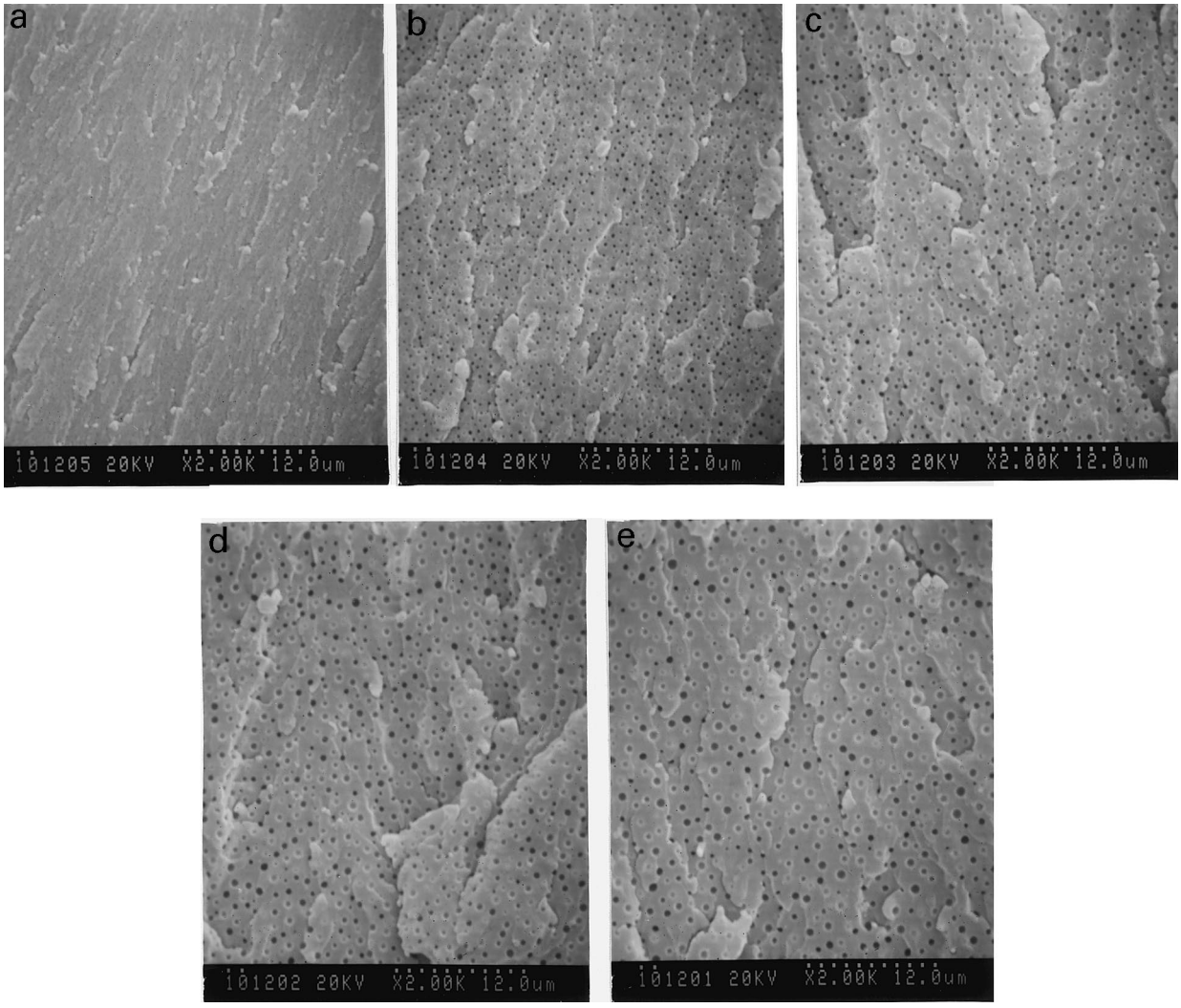

Fig. 1. SEM micrographs taken on the fractured surfaces of the PCL9 blends cured at: (a) 130°C; (b) 140°C; (c) 150°C; (d) 160°C; and (e) 170°C.

between the initiation and end of phase separation at higher curing temperature is longer than that at lower curing temperature. The observed larger PCL domain size of the PCL9 blend cured at higher temperature (Fig. 1) can be interpreted as lower epoxy conversion needed to initiate phase separation, and the PCL domain can grow larger in longer conversion interval before the termination of the phase separation.

3.3. Cured morphologies of the PCL12 and PCL15 blends

Fig. 2a and b display the PCL-rich particles dispersed in the PCL12 blends, implying that the PCL phase separation follows the NG mechanism at 130°C (Fig. 2a) and 140°C (Fig. 2b). The PCL-rich particle size at 140°C (Fig. 2b) is larger than that at 130°C (Fig. 2a), which is consistent to the tendency observed in the PCL9 blend system (Fig. 1). When the PCL12 blend is cured at 150°C or above (Fig. 2c–e), the PCL-rich macrophase with irregular shape is formed which contains numerous epoxy micro-particles. These morphologies imply that the epoxy phase separation follows the SD mechanism as illustrated in Scheme 2. Thus the critical points in terms of PCL fraction of the phase separation diagram at 130 and 140°C are located at higher than 12% PCL, while the critical points at 150°C and above are located at lower than the PCL12. On the other hand, the domain size of the epoxy micro-particles within the PCL-rich macrophase (Fig. 2c–e) increases with the increase of the curing temperature, while those PCL micro-particles (cannot be observed in 200×) within the epoxy-rich macrophase remain nearly constant regardless of the curing temperature. Similar results are also observed in the PCL15 blends (Fig. 3), in which the NG mechanism of PCL occurs only at 130°C curing temperature.

3.4. The kinetic effect

Table 1 summarizes the mechanisms of phase separation in all blends at different curing conditions. The PCL-rich particle diameters resulted from the NG mechanism of PCL,

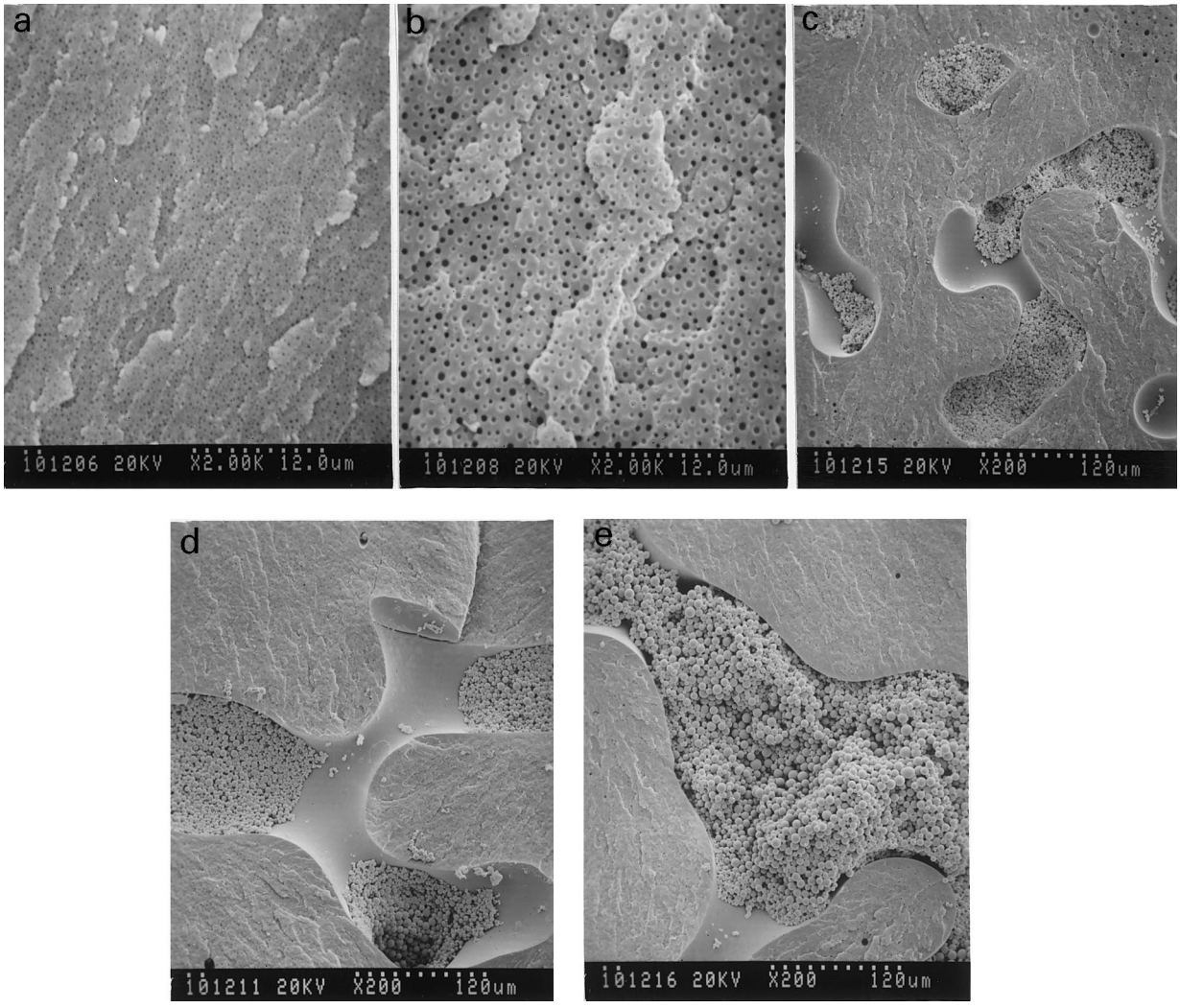

Fig. 2. SEM micrographs taken on the fractured surfaces of the PCL12 blends cured at: (a) 130°C; (b) 140°C; (c) 150°C; (d) 160°C; and (e) 170°C.

as well as the domain diameters of the micro-particles within both macrophases resulted from the SD mechanism are also listed in Table 1. In the PCL9 blends, the PCL-rich domain size resulted from the NG mechanism increases with the increase of the curing temperature (A_{130} to A_{170} in Table 1). In the blends resulted from the SD mechanism of the epoxy (B_{150}–B_{170} and C_{140} to C_{170} in Table 1), the area fraction of the PCL-rich macrophase (listed in the parenthesis) increases with the increase of the curing temperature in both PCL12 and PCL15 blends. From the SD mechanism of the epoxy as shown in Scheme 2C–F, higher fraction of the PCL-rich macrophase implies that the blend is halted in the stage of phase separation earlier than the blend composed of lower fraction of the PCL-rich macrophase. Thus higher curing temperature results in the stages of macrophase separation earlier than lower curing temperature does, which can be attributed to the kinetic effect promoted by higher temperature. On the other hand, the epoxy micro-particles within the PCL-rich macrophase exhibit larger domain size at higher curing temperature (B_{150}–B_{170} and C_{140}–C_{170} in Table 1). This phenomenon is consistent with the LCST behavior, and the kinetic effect is less or not involved in the growth of the epoxy micro-particles. The domain size of the PCL micro-particles within the epoxy-rich macrophase remains nearly constant regardless of the curing temperature. The PCL fraction and polydispersity in the epoxy-rich macrophase segregated in various stages (Scheme 1) are different from those in the original blend before phase separation [7], which cannot be characterized only by SEM. Thus, the factors that influence the domain size of the PCL micro-particles within the epoxy-rich macrophase cannot be discussed in this study. The kinetic effect only works on the growth of macrophases, which is resulted from the long-distance diffusion of both components [6]. The domain size growing tendency of the PCL phase from the NG mechanism is not influenced by the curing rate (A_{130}–A_{170} in Table 1), which means that the short-distance diffusion can be achieved more easily, and the kinetic effect does not change the domain size growing tendency.

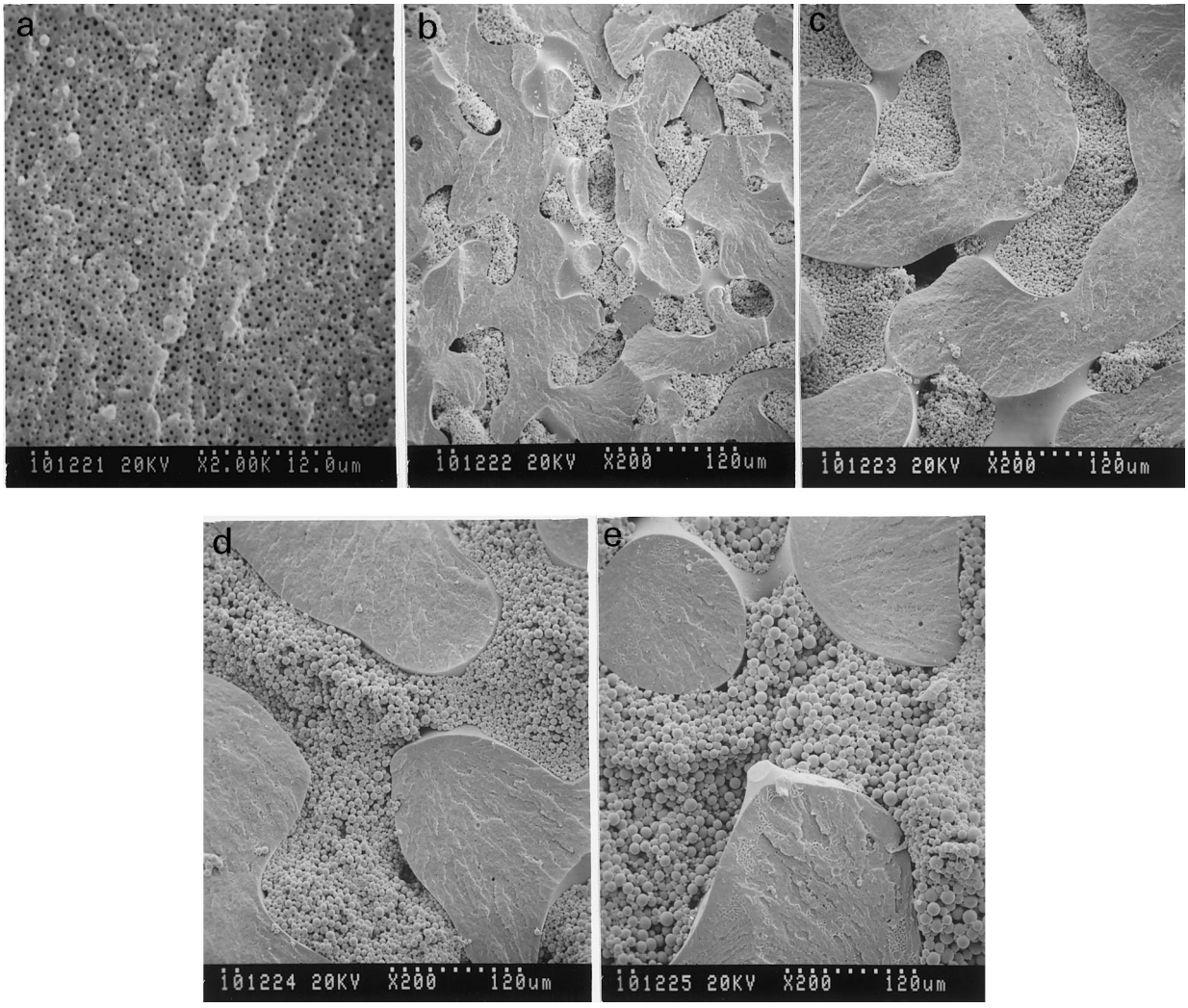

Fig. 3. SEM micrographs taken on the fractured surfaces of the PCL15 blends cured at: (a) 130°C; (b) 140°C; (c) 150°C; (d) 160°C; and (e) 170°C.

3.5. Phase diagram

Table 1 also indicates the shift of the critical point (in terms of PCL content) with curing temperature. At 130°C curing temperature, the phase separation from PCL9 to PCL15 blends proceeds via the NG mechanism of the PCL, implying that the critical point is located at higher than 15% PCL. At 140°C curing temperature, the mechanism of phase separation shifts from the NG of PCL (B_{140} in Table 1) to the SD of the epoxy (C_{140} in Table 1), indicating that the critical point is located at between 12% PCL and 15% PCL compositions. Similar results are also obtained at 150–170°C curing temperatures. The transition of phase separation mechanism is located at PCL11 composition cured at 150°C [6]. Thus the phase diagram can be drawn as Fig. 4. Three pairs of the spinodal and binodal curves represent the epoxy conversion of phase separation at 130, 140, and 150°C curing temperatures. According to the LCST behavior, phase separation at higher curing temperature should be initiated at a lower conversion. Thus, the conversion of phase separation taking place should decrease with the increase of the curing temperature as shown in Fig. 4. When the conversion grows higher than the binodal curve, phase separation takes place and terminates when the mixture viscosity reaches very high, gelation, or vitrification. In order to explain the phase separation behavior in terms of composition and percent epoxy conversion, firstly we assume the phase separation is terminated at vitrification. Again we also assumes the binodal curve at 130°C intersects with the vitrification line ($p = p_{\text{vitri}}$) with compositions at $w_1 = w_a$ and $w_1 = w_b$. Theoretically, phase separation is possible in the $w_a < w_1 < w_b$ range. The phase separation of the blend with composition $w_1 < w_a$ and $w_1 > w_b$ is thermodynamically feasible at higher conversion ($>p_{\text{vitri}}$). However, vitrification completely inhibits component diffusion for phase separation. In reality, phase separation may already been terminated before reaching its vitrification. Phase separation may be terminated when the viscosity reaches a critical level or at gelation, and the phase separation is retarded before vitrification in

Table 1
Phase separation mechanisms in all blends and curing conditions, area fraction of macrophase, and the domain diameters of spherical phases

	Curing temperature (°C)							
	130	140		150		160		170	
PCL9	A_{130}: homogeneous at 2000X	A_{140}: NG of PCL[a]		A_{150}: NG of PCL		A_{160}: NG of PCL		A_{170}: NG of PCL	
		PCL phase[b] 0.26[c]		PCL phase 0.34		PCL phase 0.48		PCL phase 0.52	
PCL12	B_{130}: NG of PCL	B_{140}: NG of PCL		B_{150}: SD of epoxy (30/70)[d]		B_{160}: SD of epoxy (42/58)		B_{170}: SD of epoxy (48/52)	
	PCL phase	PCL phase		Epoxy micro-particle	PCL micro-particle	Epoxy micro-particle	PCL micro-particle	Epoxy micro-particle	PCL micro-particle
	0.26	0.51		4.46	0.78	5.83	0.80	7.20	0.73
PCL15	C_{130}: NG of PCL	C_{140}: SD of epoxy (34/66)		C_{150}: SD of epoxy (40/60)		C_{160}: SD of epoxy (50/50)		C_{170}: SD of epoxy (60/40)	
	PCL phase	Epoxy micro-particle	PCL micro-particle	Epoxy micro-particle	PCL micro-particle	Epoxy micro-particle	PCL micro-particle	Epoxy micro-particle	PCL micro-particle
	0.36	2.74	0.50	4.11	0.50	5.83	0.62	11.86	0.59

[a] Phase separation mechanism.
[b] Spherical phase.
[c] Domain diameter (in micron) of the spherical phase.
[d] Area fraction ratio of the PCL-rich/epoxy-rich macrophase domain estimated by the SEM morphology.

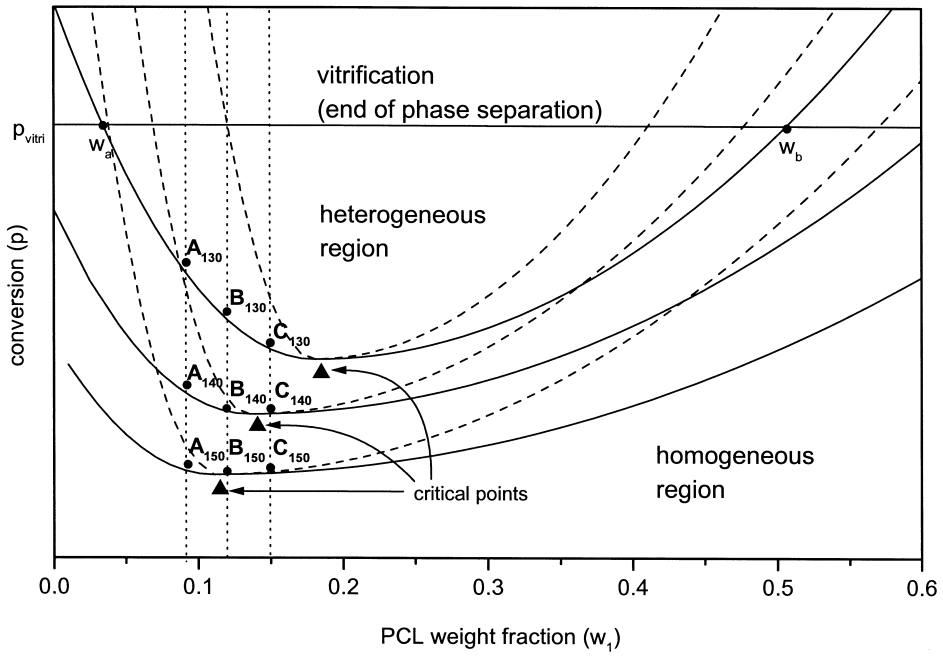

Fig. 4. Phase diagram constructed by the binodal and spinodal curves at 130, 140, and 150°C.

this study. The exact cause for phase separation termination can be achieved through carefully designed experiment that is beyond the scope of this study.

4. Conclusions

The cured morphologies depend on the blend compositions and curing conditions. Phase separation mechanism varies with curing temperature because of the location shift of the critical point on phase diagram. The curing temperature also influences the domain size of dispersed phase. The domain size in microns diameter increases with the increase of curing temperature, which is consistent to the LCST behavior. In contrast, the epoxy-rich macrophase resulted from the SD mechanism grows further at lower temperature. This phenomenon can be attributed to the kinetic effect that only works on the long-distance diffusion resulting in the macrophase. The kinetic effect is less or not involved in the growth of the micro-particles through the short-distance diffusion. The morphological evolution can be illustrated by the phase diagram constructed by the binodal and spinodal curves. According to the LCST behavior, the conversion of phase separation initiation should decrease with the increase of curing temperature. The location of the critical point also shifts to lower PCL fraction when the curing temperature is increased. When the binodal curve intersects with some critical conversion of phase separation termination at two intersections, the homogeneous blends should be achieved outside the PCL fraction interval between the intersections. This kind of homogeneous blend is resulted from the phase separation retarded to beyond the critical conversion inhibiting the phase separation, which is not feasible in thermodynamics.

Acknowledgements

This research is financially supported by the National Science Council, Taiwan, ROC under the contact No. NSC 89-2216-E-009-004. We thank Epolab Chemical Co. for material donation.

References

[1] Kim BS, Chiba T, Inoue T. Polymer 1993;34:2809.
[2] Verchere D, Sautereau H, Pascault J-P, Moschiar SM, Riccardi CC, Williams RJJ. In: Riew CK, Gillham JK, editors. Toughened plastics I, Adv. Chem. Ser. 233. Washington, DC: American Chemical Society, 1993. p. 335–63.
[3] Teng KC, Chang FC. Polymer 1993;34:4291.
[4] Girard-Reydet E, Sautereau H, Pascault JP, Keates P, Navad P, Thollet G, Vigier G. Polymer 1998;39:2269.
[5] Kim BS, Chiba T, Inoue T. Polymer 1989;60:1839.
[6] Chen JL, Chang FC. Macromolecules 1999;32:5348.
[7] Williams RJJ, Rozenberg BA, Pascault J-P. Adv Polym Sci 1997;128:95.
[8] Kammer HW, Inoue T, Ougizawa T. Polymer 1989;30:888.
[9] Kammer HW, Kressler J, Kummerloewe C. Adv Polym Sci 1993;106:31.
[10] Chen JL, Huang HM, Li MS, Chang FC. J Appl Polym Sci 1999;71:75.
[11] Clark JN, Daly JH, Garton A. J Appl Polym Sci 1984;29:3381.
[12] Garton A. Polym Engng Sci 1983;23:663.